https://doi.org/10.5194/egusphere-2026-1805
Preprint. Discussion started: 20 April 2026

Extreme Extratropical Cyclones in a Warmer Climate: Assessing Signal Robustness and Model Uncertainty

Lara C. Mercier[1], Hilla Afargan-Gerstman[2], Matthew D. K. Priestley[3], Jens H. Christensen[4], and Daniela I.V. Domeisen[5,1]

[1]Institute for Atmospheric and Climate Science, ETH Zurich, Zurich, Switzerland
[2]Oeschger Centre for Climate Change Research, Institute of Geography, University of Bern, Bern, Switzerland
[3]Department of Mathematics and Statistic, University of Exeter, Exeter, UK
[4]Physics of Ice, Climate and Earth, Niels Bohr Institute, University of Copenhagen, Copenhagen, Denmark,
[5]Faculty of Geosciences and Environment, University of Lausanne, Lausanne, Switzerland

Correspondence: Lara C. Mercier (mercierl@ethz.ch) and Hilla Afargan-Gerstman (hilla.gerstman@unibe.ch)

Abstract. Extratropical cyclones (ETCs) are the primary drivers of severe weather over the North Atlantic, yet projections of changes in the intensity of the most extreme storms remain highly uncertain. This study investigates inter-model uncertainty in future climate projections of extreme cyclones in winter, arising from competing processes such as reduced midlatitude baroclinicity and enhanced moisture availability. We analyze the future changes in the most intense 100 ETCs across 13 models from the Coupled Model Intercomparison Project Phase 6 (CMIP6) under the highest forcing scenario (SSP5-8.5). Results show a robust increase in 850 hPa relative vorticity found in 11 of 13 models, signaling an intensification of extreme cyclones despite reduced baroclinicity (9/13 models). Precipitation associated with extreme cyclones intensifies (11/13 models) despite near surface temperature gradient weakening, with results suggesting that the weakening of dry baroclinic processes is offset by enhanced diabatic feedbacks. Surface winds show no consensus, highlighting the large variability across models in predicting cyclone-related winds. Spatially, extreme storms in the North Atlantic tend to exhibit an eastward shift towards Europe (7/13 models), with mixed latitudinal responses. Overall, these findings show a projected intensification of extreme midlatitude cyclones in the North Atlantic, accompanied by robust thermodynamic signals related to an intensified precipitation in most models. Further assessments utilising large ensembles of climate models, alongside systematic investigations of extreme cyclone energetics can help to further clarify the relative importance of dry baroclinic versus moist diabatic processes.

1 Introduction

Climate models are essential tools for understanding present and future variability in midlatitude storm tracks and the behavior of extratropical cyclones (ETCs). The latest generation of climate models has provided important insights into North Atlantic cyclone characteristics, but substantial challenges remain. Previous analyses of climate model simulations from the fifth and the sixth phases of the Coupled Model Intercomparison Project (CMIP) have shown persistent biases in the representation of ETCs, including overly zonal storm track extension into Europe, underestimated cyclone counts, and insufficient representation of the most intense systems (Zappa et al., 2013; Chang, 2016; Priestley et al., 2023). These biases have been linked to model

https://doi.org/10.5194/egusphere-2026-1805
Preprint. Discussion started: 20 April 2026

resolution limitations, misrepresentation of oceanic frontal zones and air-sea interactions, and deficiencies in moist physics parameterizations. Specifically, these processes affect projections of future storm track changes, which show large inter-model spread in both magnitude and spatial patterns, especially in winter (Catto et al., 2019). Multi-model mean fields often smooth over substantial inter-model disagreement because individual models produce distinct spatial patterns, magnitudes, and even opposing signs of projected change. These differences arise from variations in how key processes such as diabatic heating, moisture transport, and storm-track–circulation coupling are represented(Zappa et al., 2013; Catto et al., 2019; Priestley et al., 2023).

Multiple physical drivers govern future ETC behavior under increased greenhouse gas emissions. These drivers include arctic amplification, tropical amplification, and stratospheric polar vortex changes (Zappa and Shepherd, 2017; Oudar et al., 2020; Manzini et al., 2014; Karpechko et al., 2022). In the lower-troposphere, arctic amplification weakens meridional temperature gradients, and therefore baroclinicity, which represents the primary energy source for cyclone growth through dry baroclinic instability (Screen and Simmonds, 2014; Vallis, 2007). At the same time, warming increases atmospheric moisture and enhances latent heat release in ascending airstreams, strengthening diabatic processes that can intensify cyclone circulation (Laïne et al., 2009; Pfahl et al., 2015c; Binder et al., 2023; Shaw et al., 2016). Enhanced moisture fuels greater condensation, stronger vertical motion, and diabatically generated potential vorticity anomalies, which may increasingly dominate the most extreme ETCs under warming (Pfahl et al., 2015c; Binder et al., 2023; Zeitzen et al., 2025). While these arguments apply to the mean state; synoptic systems may still locally encounter strong gradients, and diabatic processes may increasingly dominate extreme cyclones in a warmer climate. Understanding how these competing mechanisms shape ETCs, particularly their most extreme events, therefore remains an open research question.

Future projections consistently show a decrease in total Northern Hemisphere ETC frequency of about 5–10 percent under strong warming scenarios (Catto et al., 2019; Priestley and Catto, 2022a). However, changes in cyclone intensity are far less certain and strongly depend on the metric used: relative vorticity, minimum pressure, wind speed, or precipitation can yield different signals (Zappa et al., 2013; Catto et al., 2019). Notably, intense ETCs are responsible for the most severe wind damage, heavy precipitation, and coastal impacts (Pfahl et al., 2015c; Binder et al., 2023; Zeitzen et al., 2025), making their future evolution particularly relevant for risk assessment (Pinto et al., 2007; Severino et al., 2024; Little et al., 2023). Moreover, while typical ETCs may weaken due to reduced baroclinicity, the upper tail of the intensity distribution may undergo different changes and can intensify because of strengthened diabatic amplification (Pfahl et al., 2015c; Priestley and Catto, 2022a). A further complication is in the strong inter-model variability in future projections, with different models projecting wide arrays in the magnitude, spatial pattern, and even the sign of projected changes in both intensity and storm track position.

Despite a general consensus as to how the intensity of the most extreme North Atlantic ETCs will change across CMIP6 models, it is uncertain how the role of the environments surrounding these storms may influence this change, and how inter-model uncertainty manifests in the thermodynamic and dynamic aspects of cyclone intensification.

In this study, we address these gaps by investigating the future changes of the top 100 most intense ETCs in 13 CMIP6 models under the SSP5-8.5 scenario using a Lagrangian storm track perspective. We assess changes in midlatitude cyclone intensity (850 hPa relative vorticity), thermodynamic structure (precipitation), near-surface temperature gradients (as a proxy

https://doi.org/10.5194/egusphere-2026-1805
Preprint. Discussion started: 20 April 2026

for baroclinicity), and surface wind speed across the models. We further analyze longitudinal and latitudinal shifts in the location of peak intensity for extreme ETCs and evaluate the degree of inter-model agreement across all aspects. This combined dynamical–thermodynamical framework is designed to identify which projected changes are robust across models and which remain dominated by structural uncertainty. This framework provides a multi-variable, process-based perspective on how extreme ETCs may evolve under strong warming and clarifies which projected changes are robust and which remain uncertain.

2 Data and Methods

2.1 CMIP6 Models

This study uses 13 climate models from the Coupled Model Intercomparison Project Phase 6 (CMIP6), detailed in Table 1. Model selection was based on two criteria: (1) availability of the required daily surface variables (precipitation, 2-meter air temperature, and 10-meter wind components) for both historical and future periods, and (2) availability of variables at a 6-hourly temporal resolution for cyclone tracking following the method applied in Priestley and Catto (2022a).

Model	Institution	Resolution (lon × lat)	Levels
ACCESS-CM2	CSIRO-ARCCSS, Australia	1.875° × 1.25°	85
BCC-CSM2-MR	BCC, China	1.125° × 1.125°	46
CMCC-CM2-SR5	CMCC, Italy	1.0° × 1.0°	30
CMCC-ESM2	CMCC, Italy	1.0° × 1.0°	30
EC-Earth3	EC-Earth Consortium, Europe	0.7° × 0.7°	91
KIOST-ESM	KIOST, South Korea	1.875° × 1.875°	32
MIROC6	MIROC, Japan	1.4° × 1.4°	81
MPI-ESM1-2-HR	MPI-M, Germany	0.94° × 0.94°	95
MPI-ESM1-2-LR	MPI-M, Germany	1.875° × 1.875°	47
NESM3	NUIST, China	1.875° × 1.875°	47
NorESM2-LM	NCC, Norway	2.5° × 1.875°	32
NorESM2-MM	NCC, Norway	1.25° × 0.9375°	32
TaiESM1	AS-RCEC, Taiwan	1.25° × 0.9375°	30

Table 1. Characteristics of the 13 CMIP6 models used in this study. Resolution refers to the nominal atmospheric grid spacing (longitude × latitude), and Levels indicates the number of vertical levels in the atmospheric component.

2.2 Reanalysis data

For comparison of climate model output against the observed climatology, we use fifth generation ECMWF atmospheric reanalysis (ERA5) of the global climate covering the period from December 1980 to 2010. We use relative vorticity at 850 hPa data, with a temporal resolution of 6 h at a 0.25° spatial resolution (Hersbach et al., 2020).

https://doi.org/10.5194/egusphere-2026-1805
Preprint. Discussion started: 20 April 2026

2.3 Cyclone Tracking

Generally, midlatitude storm tracks can be represented using two different perspectives: Eulerian and Lagrangian. While the Eulerian storm perspective is based on bandpass time-filtering of meteorological fields (e.g., Blackmon, 1976; Hoskins and Valdes, 1990), Lagrangian storm track perspective allows to identify synoptic features and track them throughout their life cycle (e.g., Hodges, 1994; Wernli and Schwierz, 2006).

In this study, extratropical cyclones in CMIP6 models were identified and tracked using the Lagrangian feature-tracking method described by Hodges (1994, 1995, 1999). This widely-used algorithm identified cyclones as maxima in the 850 hPa relative vorticity field on a 6-hourly temporal resolution and tracks them throughout their life cycle, from genesis to decay.

To ensure consistency across models with varying native resolutions and to focus on synoptic-scale cyclones, the vorticity field was spectrally truncated to T42 ($\sim$2.8° equivalent resolution) before tracking. Additionally, large-scale planetary waves were removed by filtering out total wavenumbers ≤ 5 in spectral space. This isolates synoptic-scale disturbances (wavelengths of approximately 1000–5000 km) relevant to extratropical cyclone activity while removing very large-scale features and model-dependent computational modes.

Following Priestley and Catto (2022a), only cyclone tracks satisfying three criteria were retained for analysis: (1) minimum duration of 48 hours (8 consecutive 6-hourly time steps), (2) minimum travel distance of 1000 km, and (3) maximum cyclone vorticity of $\geq$1x10^{-5} s^{-1}. These thresholds eliminate detections of short-lived vorticity maxima, stationary features, and small-scale disturbances that may not represent coherent extratropical cyclones. The resulting track database provides cyclone characteristics including location, intensity (relative vorticity), and associated meteorological fields at each 6-hourly time step throughout the cyclone lifecycle.

2.4 Extreme Event Selection

For each identified cyclone track, the maximum relative vorticity attained during the track's lifetime was extracted. For the North Atlantic analysis, only cyclones with at least 10 track points within the study domain (30°N–70°N, 80°W–20°E) were considered, with maximum vorticity required to occur within this region. This ensures focus on cyclones that develop or reach peak intensity over the North Atlantic.

To focus on the most intense cyclones, the top 100 unique highest vorticity values were identified for each model and period (historical: 1980–2010; future: 2070–2100). This approach ensures consistent sample sizes across all models and periods, facilitating direct inter-model comparison.

The choice of 100 events represents an approximately uniform proxy for the 99th percentile of cyclone intensity. Because models produce varying numbers of cyclones per 30-year period, selecting a fixed percentile would yield different sample sizes across models, complicating statistical comparison and potentially introducing sampling biases. The top-100 approach ensures all models contribute equal numbers of extreme events and the sample size is sufficiently large for robust composite statistics while focusing on extreme rather than typical cyclones. This method therefore allows for an assessment of whether the most intense cyclone characteristics change under future warming, independent of changes in overall cyclone frequency.

https://doi.org/10.5194/egusphere-2026-1805
Preprint. Discussion started: 20 April 2026

2.5 Composite Analysis

Cyclone-centered composites were constructed to examine the structural characteristics associated with the top-100 most intense cyclones in the North Atlantic. For each extreme cyclone, daily CMIP6 data for precipitation, 2-meter air temperature, and 10-meter wind speed were extracted and interpolated onto a $30° \times 30°$ grid centered on the cyclone's position at maximum vorticity, with a resolution of $0.5°$. This domain captures the cyclone core structure, including frontal zones, precipitation maxima, and wind field asymmetries.

Composites were computed by averaging gridded fields over all top-100 events for each model and period.

To capture the characteristic temporal evolution, different lags were applied relative to the time of maximum intensity:

Precipitation is composited at -1 day to capture pre-cyclone moisture convergence and the ascending warm conveyor belt phase, when latent heating and precipitation intensification contribute to cyclone development. The 10-meter wind speed is composited at +1 day, when peak near-surface winds typically occur due to downward momentum transport and strong pressure gradients as the cyclone matures. The meridional gradient of 2-meter air temperature, composited at time 0, was computed as $|\partial \text{tas}/\partial \text{lat}|$ using centered finite differences. To facilitate inter-model comparison and focus on relative changes, temperature gradient composites were standardized.

2.5.1 Statistical Significance Testing

Differences between historical and future composites were evaluated using non-parametric bootstrap resampling. For each variable and model, 1000 bootstrap samples were generated by randomly resampling (with replacement) cyclone-centered fields from the combined historical and future pool. Each sample was randomly partitioned into two groups matching the original sample sizes, and mean differences were calculated to generate a distribution under the null hypothesis of no systematic change. The 95% confidence interval was determined using the 2.5th and 97.5th percentiles of resampled differences at each grid point. Grid points where the observed difference fell outside this interval were considered significant at the 5% level ($p < 0.05$). Non-significant regions are indicated by dotting in composite figures.

This bootstrap approach requires no distributional assumptions, making it suitable for meteorological variables with skewed or heavy-tailed distributions, and accounts for sampling variability in extreme event populations.

2.6 Assessment of Shifts in Peak Intensity Location

Changes in the spatial distribution of extreme cyclones is assessed for the top-100 cyclones in each model for the historical and future periods. Longitudinal shifts are defined relative to 50°W. A model is classified as showing an eastward shift when peak-intensity counts increased east of 50°W and decreased to the west, and as showing a westward shift when counts increased west of 50°W and decreased to the east. Latitudinal shifts are defined relative to 50°N. A northward shift corresponds to increased activity north of 50°N with reduced counts to the south, whereas a southward shift corresponds to the opposite pattern. Models are classified as exhibiting a mixed response when increases and decreases occurred on both sides of the threshold without forming a coherent directional signal.

https://doi.org/10.5194/egusphere-2026-1805
Preprint. Discussion started: 20 April 2026

To test whether historical and future spatial distributions differ significantly, a two-sample Kolmogorov–Smirnov (KS) test was applied separately to the longitude and latitude samples. The KS statistic quantifies the maximum difference between the empirical cumulative distributions, and the associated p-value tests the null hypothesis that both samples originate from the same distribution. The KS test indicates whether the overall distribution changes but does not determine the direction of a shift, which is derived solely from redistribution patterns around 50°W and 50°N.

3 Results

This section synthesizes changes in the intensity, structure, and spatial distribution of extreme North Atlantic extratropical cyclones under future climate warming, combining dynamical and thermodynamical perspectives.

3.1 Multi-Model Storm Track Density

Figure 1 presents the projected changes in cyclone track density for each of the 13 CMIP6 models. Black contours show the historical climatological track density, indicating the baseline spatial pattern of cyclone activity for each model. Shaded regions represent end-of-century changes, with blue indicating decreased track density and red indicating increased.

Substantial inter-model spread is evident in both the spatial patterns and magnitudes of projected changes. Over the North Atlantic, several models (ACCESS-CM2, CMCC-CM2-SR5, CMCC-ESM2, KIOST-ESM, MIROC6, NorESM2-MM, NESM3) show a decrease in track density for a future climate over the western and central basin with increased density over northwestern Europe and the Nordic Seas. Other models (BCC-CSM2-MR, EC-Earth3, MPI-ESM1-2-LR) exhibit more heterogeneous patterns with both increases and decreases distributed across multiple regions without clear directional shifts. MPI-ESM1-2-HR and TaiESM1 show increases in the central to eastern Atlantic.

https://doi.org/10.5194/egusphere-2026-1805
Preprint. Discussion started: 20 April 2026

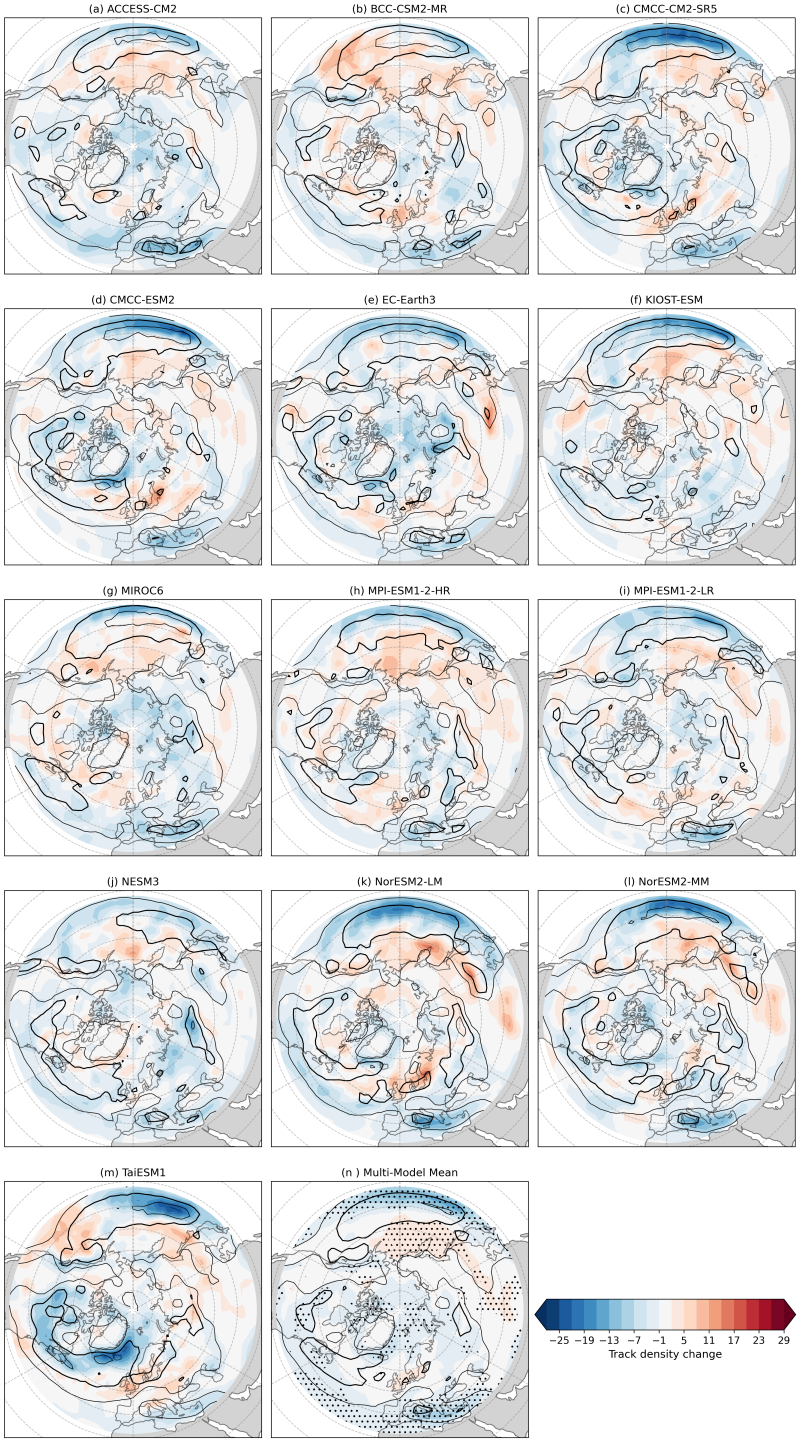

Figure 1. Future (SSP5-8.5; 2070–2100) cyclone track density changes relative to the historical period (1980–2010) for Northern Hemisphere winter (DJF) across 13 CMIP6 models. Shading indicates the change in track density (cyclones per 5° spherical cap). Black contours represent the historical climatological track density for each model. Thick contour highlight the level showing area with 60% of maximum cyclones occurrence (40 events). Stippling in panel n represents >80% model agreement. Units are cyclones per season per 5° spherical cap.

https://doi.org/10.5194/egusphere-2026-1805
Preprint. Discussion started: 20 April 2026

Table 2. Multi-Variable Model Responses (Historical to Future SSP5-8.5).

Legend: E = Eastward, W = Westward, N = Northward, S = Southward, M = Mixed

Model	Vorticity Change	Precip. Change	Wind Change	Temp. Gradient	Long. Shift	Lat. Shift
ACCESS-CM2	+3%	+50-75%	-10 to -15%	-20 to -30%	M	M
BCC-CSM2-MR	-2%	+25-50%	-5 to -10%	Dipole	W	M
CMCC-CM2-SR5	+2%	∼50%	+10-15%	-15 to -25%	E	M
CMCC-ESM2	+2%	+25-70%	+10-15%	-15 to -35%	E	M
EC-Earth3	∼0%	+40-70%	+30%+	-15 to -25%	M	M
KIOST-ESM	+3%	+25-50%	-5 to -10%	Dipole	M	M
MIROC6	+5%	+25-75%	+20%+	-30%+	E	N
MPI-ESM1-2-HR	+6.7%	Minimal	-5 to -10%	-15 to -40%	E	M
MPI-ESM1-2-LR	+2%	+25-50%	+5-10%	-15 to -40%	M	S
NESM3	-2%	+50-75%	$\sim \pm 5\%$	-15 to -35%	E	N
NorESM2-LM	+4%	+50-75%	+18%	-30%+	M	N
NorESM2-MM	+5%	+75%+	+10-18%	-15 to -25%	E	M
TaiESM1	+3%	-25 to -50%	+5-12% / -15%	Mixed	E	S
Multi-Model Mean	N/A	+20%	-20%	Minimal	M	M

3.2 Changes in cyclone vorticity in CMIP6 projections

Figure 2 shows the response of peak cyclone relative vorticity, with 11 of 13 models showing an increase in the SSP5-8.5 scenario relative to the historical period, indicating stronger lower-tropospheric circulation in extreme cyclones. The largest relative increase occurs in MPI-ESM1-2-HR (+6.7%), closely followed by MIROC6 and NorESM2-MM (+5% each). Two models show decreases: BCC-CSM2-MR and NESM3 (both -2%). Table 2 summarizes the model responses for vorticity, precipitation, surface wind and temperature gradient associated with the extreme cyclones.

To verify the range of extreme cyclone vorticity values in the historical simulations, these values are compared against the observed range in ERA5 reanalysis. The historical model values span from $0.00013\ \mathrm{s}^{-1}$ to $0.00016\ \mathrm{s}^{-1}$, encompassing the ERA5 magnitude of approximately $0.000126\ \mathrm{s}^{-1}$, confirming that the models represent realistic baseline intensities. The

https://doi.org/10.5194/egusphere-2026-1805
Preprint. Discussion started: 20 April 2026

clustering of most models above the 1:1 identity line (Figure 2) across this range of baseline intensities indicates a consistent strengthening signal.

The lower panel examines intra-model variability using 15 members of the MPI-ESM1-2-LR large ensemble, providing a large set of realizations to assess internal climate variability within a single model. While the main analysis relies on the first ensemble member of each CMIP6 model for consistency across models, analysing all 15 members here allows us to test the robustness of the projected changes against internal variability. 12 out of 15 members display mean vorticity increases from the historical to the SSP5-8.5 periods, with values clustering tightly around $0.00014\ \mathrm{s}^{-1}$ for both periods. The consistency across ensemble members confirms that the projected intensification signal exceeds internal climate variability within this model.

The range of vorticity values in the multi-model comparison indicate substantial variation in individual extreme events (horizontal and vertical lines extending from each marker).

Inter-model agreement is strongest for the sign of the future change in cyclone intensity, while the magnitude remains highly uncertain. This spread likely reflects differences in model resolution, representation of baroclinic growth, and sensitivity of cyclone dynamics to lower-tropospheric changes. Importantly, mean-state biases alone is not the sole factor controlling projected extreme cyclone changes, as also demonstrated by the weak correlation with present-day cyclone activity.

3.3 Changes in cyclone environment

To better understand how extreme ETC structure responds to warming, we analyze cyclone-centered composites of precipitation, near-surface temperature gradients, and surface wind speed for the top-100 most intense cyclones in each model. These composites provide a physically grounded view of the thermodynamic and dynamic environments in which extreme cyclones reach maximum intensity, complementing the vorticity-based intensity changes discussed above. Figures 3, 4, and 5 show the model-by-model cyclone-centered responses for precipitation, standardized temperature gradients, and surface winds, respectively, together with the multimodel mean (MMM).

3.3.1 Precipitation Changes

Figure 3 presents cyclone-centered composite maps of precipitation change expressed as percentage shift relative to the historical baseline of each model, as well as the multimodel mean (MMM). Across the ensemble, 11 out of 13 models exhibit increased precipitation near the cyclone center. The strongest and most statistically robust increases occur within approximately 2°–3° of latitude and longitude around the cyclone center in both the individual-model panels and the MMM. A few models, however, display regional decreases or mixed signals around the periphery. The MMM also highlights areas where at least 80% of the models agree on the sign of change (indicated by non-shading in the bottom-right panel), emphasizing that the most robust response is the central precipitation intensification. Pfahl et al. (2015b) demonstrated that enhanced latent heating in the warm conveyor belt creates positive feedbacks that strengthen cyclone circulation, which in turn enhances moisture convergence and further amplifies precipitation. Taken together, these results indicate that enhanced latent heating is a consistent and robust feature of future extreme ETCs across the CMIP6 models.

https://doi.org/10.5194/egusphere-2026-1805
Preprint. Discussion started: 20 April 2026

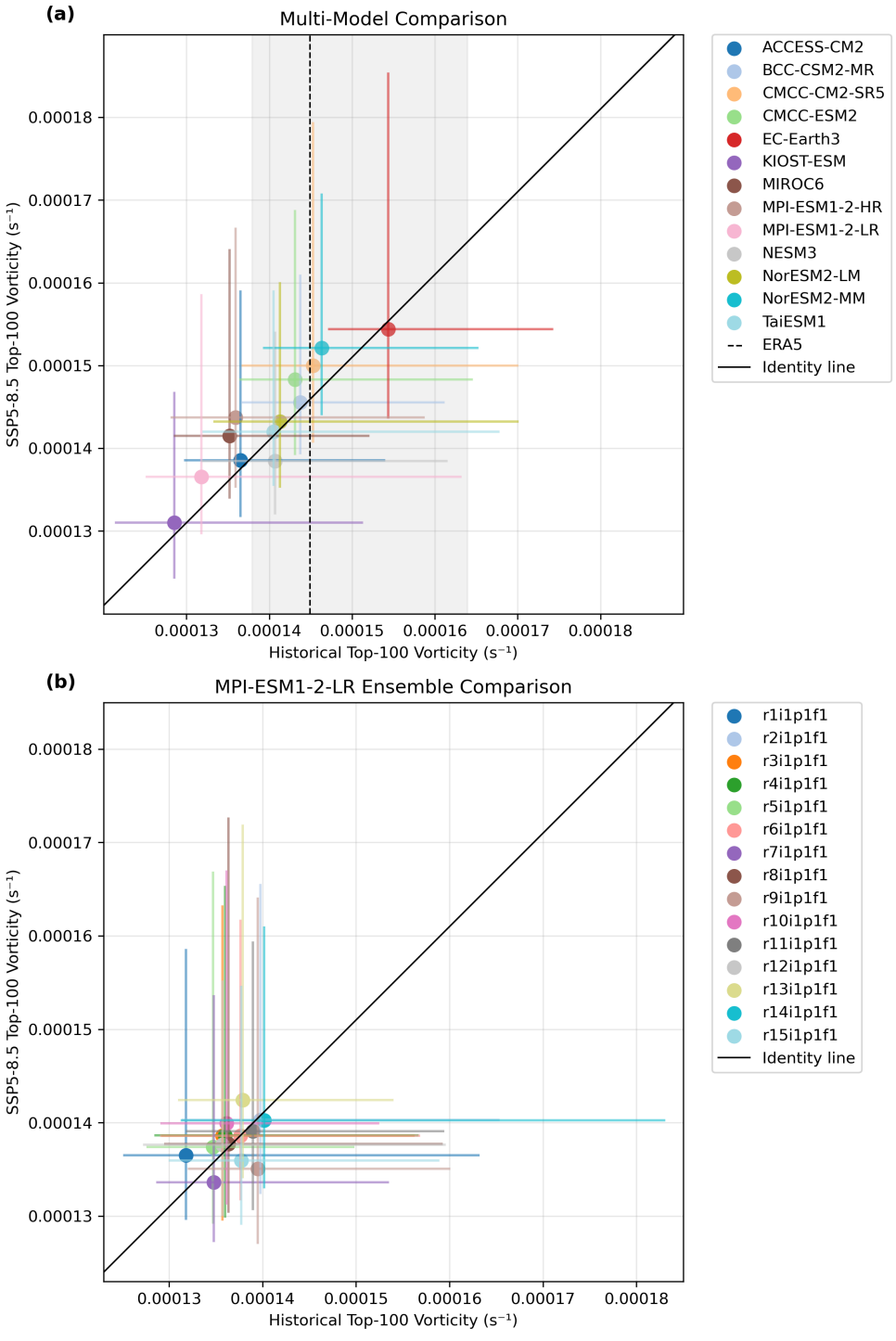

Figure 2. a) Multi-model comparison of mean top-100 vorticity values between the historical period (1980–2010) and future SSP5-8.5 scenario (2070–2100 for 13 CMIP6 models over the North Atlantic. Colored markers represent individual models, with horizontal and vertical lines indicating the range (minimum to maximum) of vorticity values within each model's top-100 events. The dashed black line represents the 1:1 identity line. b) Same as panel a), but for an intra-model comparison of 15 ensemble members of MPI-ESM1-2-LR.

https://doi.org/10.5194/egusphere-2026-1805
Preprint. Discussion started: 20 April 2026

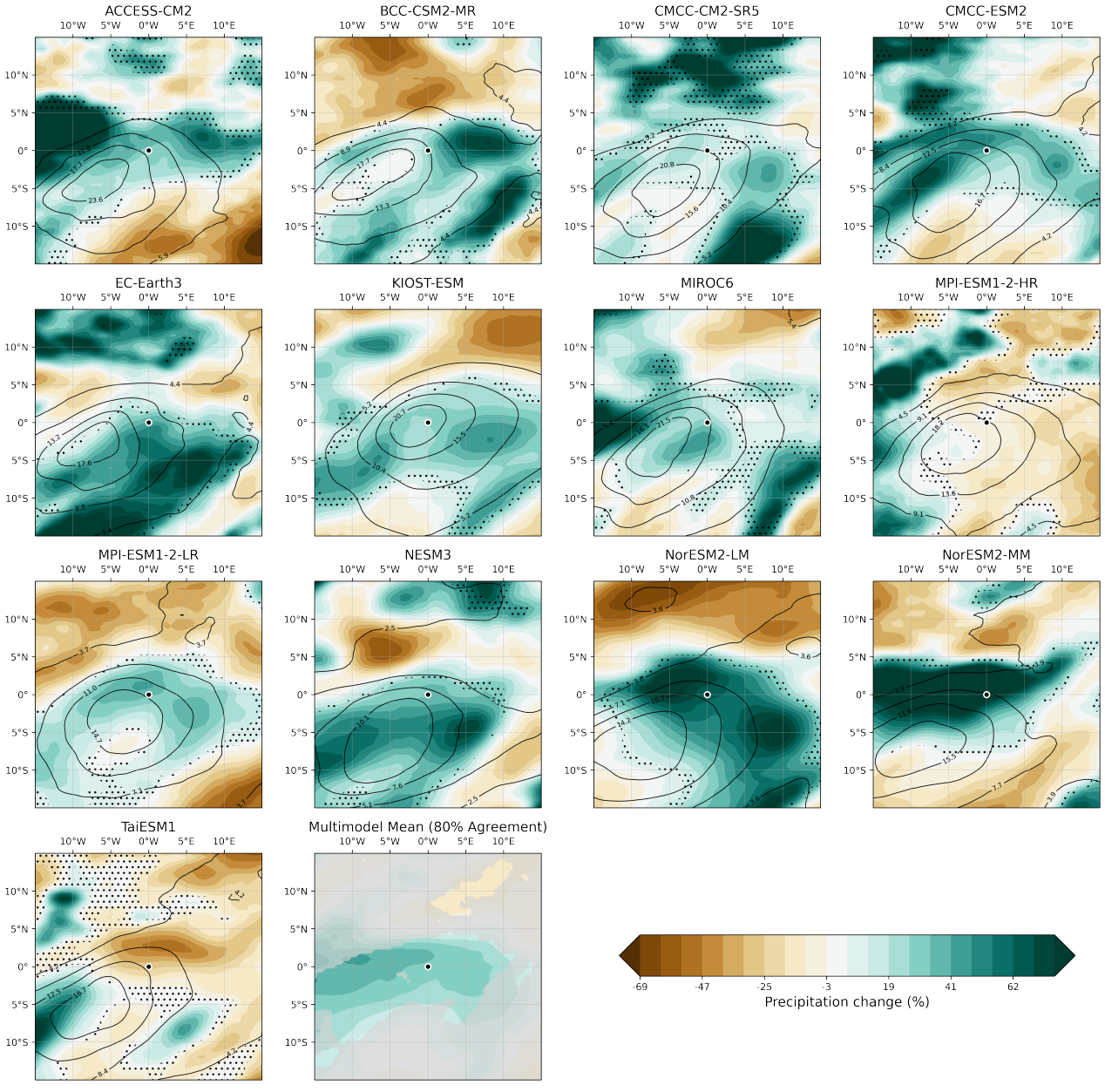

Figure 3. Cyclone-centered composite maps of percentage change in precipitation between SSP5-8.5 (2070–2100) and historical (1980–2010) periods for 13 CMIP6 models. The bottom-right panel shows the multimodel mean (MMM); shaded regions show where less than 80% of models agree on the sign of change. The cyclone center is marked with a black dot. Each subplot shows a $30^\circ \times 30^\circ$ domain centered on the cyclone center, with longitude on the x-axis and latitude on the y-axis. Dots indicate regions without statistical significance at the 5% level.

https://doi.org/10.5194/egusphere-2026-1805
Preprint. Discussion started: 20 April 2026

3.3.2 Surface Temperature Gradient Changes

Figure 4 presents cyclone-centered composite maps of percentage change in standardized surface temperature latitudinal gradient. The spatial patterns show both regions of strengthening and weakening temperature gradients across the model domain. Most models project a weakening of the near-surface temperature gradient around cyclones, and particularly to the northeast of the cyclone center. While several models display widespread decreases exceeding 20–30%, others show mixed or dipole-like structures, with local strengthening on one side of the cyclone. Overall, the ensemble suggests that future cyclones may evolve in an environment with weaker horizontal temperature contrasts. The largest decreases in gradient across the models lies to the NW of the cyclone center (reductions of 20–40%) and provides robust evidence that extreme cyclones will develop in environments with reduced low-level baroclinicity. This reduction is fundamentally driven by Arctic amplification, where high-latitude regions warm faster than lower latitudes (Screen and Simmonds, 2014).

It is notable that the precipitation enhancement occurs despite widespread reductions in surface temperature gradients. Models showing strong precipitation increases alongside reduced baroclinicity include ACCESS-CM2 (50–75% precipitation increase, 20–30% temperature gradient decrease), NorESM2-LM (50–75% precipitation increase, exceeding 30% temperature gradient decrease), MIROC6 (25–75% precipitation increase, exceeding 30% temperature gradient decrease), and NESM3 (50–75% precipitation increase, 15–35% temperature gradient decrease) as summarized in Table 2. This coexistence directly demonstrates the transition from dry baroclinic to moist diabatic dynamics in extreme cyclones in a warming climate (Binder et al., 2023; Pfahl et al., 2015a).

Classical baroclinic instability theory predicts that reduced temperature gradients should weaken cyclone intensity (Vallis, 2007). The fact that our ensemble shows vorticity increases in 11 out of 13 models despite widespread temperature gradient reductions indicates that latent heat release is compensating for and potentially overriding the dynamical weakening from reduced baroclinicity in these extreme cyclones and therefore represents a fundamental shift in the physics governing extreme cyclone development.

3.3.3 Surface Wind Speed Changes

Figure 5 displays cyclone-centered composite maps of percentage change in surface horizontal wind speed. The patterns show considerable diversity across the model ensemble in terms of both spatial structure and magnitude of changes. Changes in surface wind speed show the greatest model-to-model variability among the three examined variables so far. Roughly half of the models project strengthening near the cyclone core or in the surrounding areas, while the rest of the models show widespread or partial weakening. The ensemble does not exhibit a consistent wind speed trend in the MMM, implying that circulation changes are highly model dependent and may reflect differing responses in storm structure and intensity. This contrasts with (Priestley and Catto, 2022a), who found robust strengthening in the rear flank and warm sector when analyzing winds at 850 hPa (their Fig. 6j). The difference suggests that near-surface winds are strongly influenced by boundary-layer friction, turbulent mixing, and surface drag, which act to damp and redistribute momentum, leading to much greater inter-model variability at surface than aloft. Moreover, model resolution has a substantial impact on the representation of near-surface wind maxima in intense

https://doi.org/10.5194/egusphere-2026-1805
Preprint. Discussion started: 20 April 2026

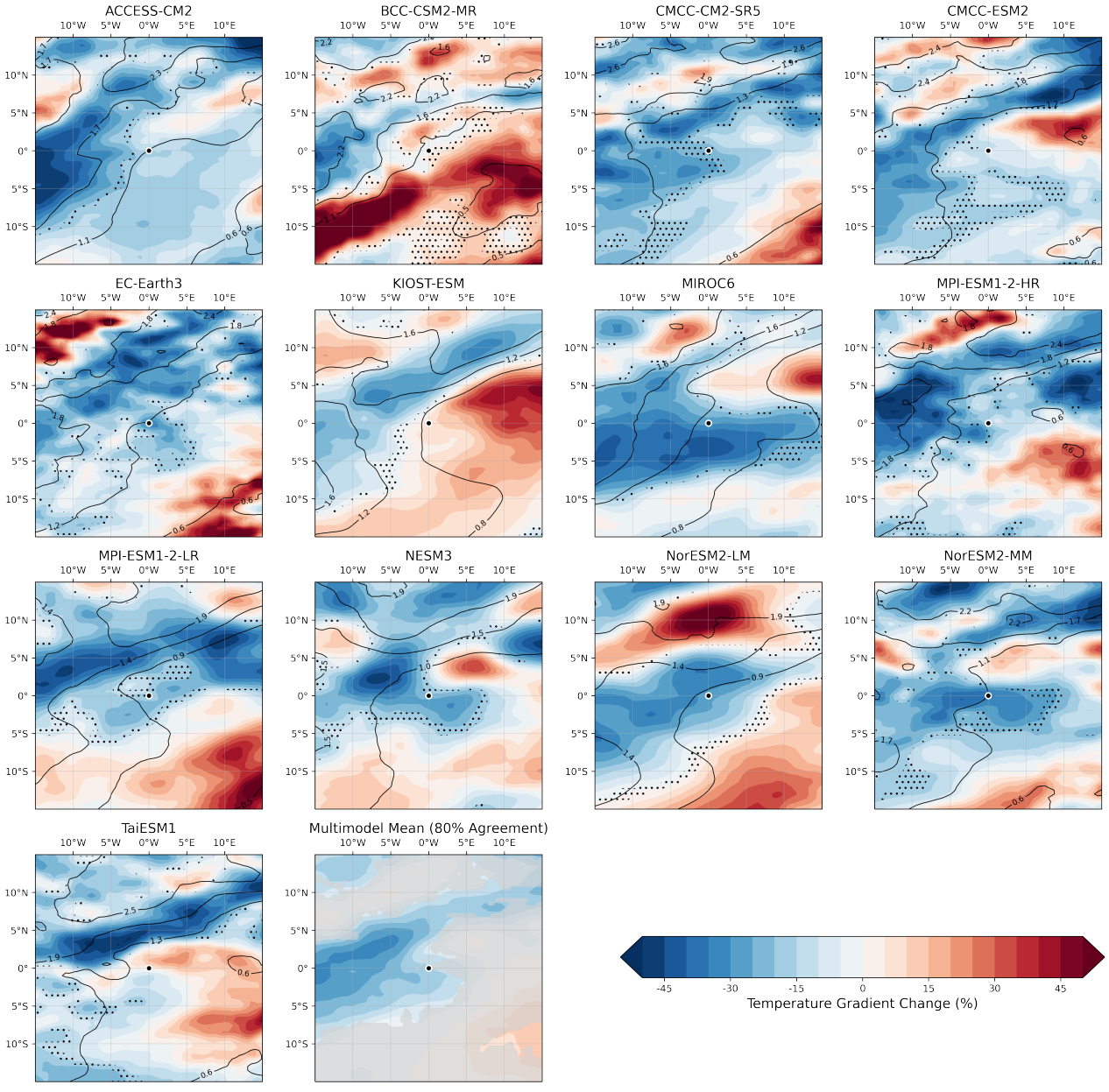

Figure 4. Cyclone-centered composite maps of percentage change in standardized surface temperature gradient between SSP5-8.5 (2070–2100) and historical (1980–2010) periods for 13 CMIP6 models. The bottom-right panel shows the multimodel mean (MMM); shaded regions show where less than 80% of models agree on the sign of change. The cyclone center is marked with a black dot. Each subplot shows a $30^\circ \times 30^\circ$ domain centered on the cyclone, with longitude on the x-axis and latitude on the y-axis. Dots indicate regions without statistical significance at the 5% level.

https://doi.org/10.5194/egusphere-2026-1805
Preprint. Discussion started: 20 April 2026

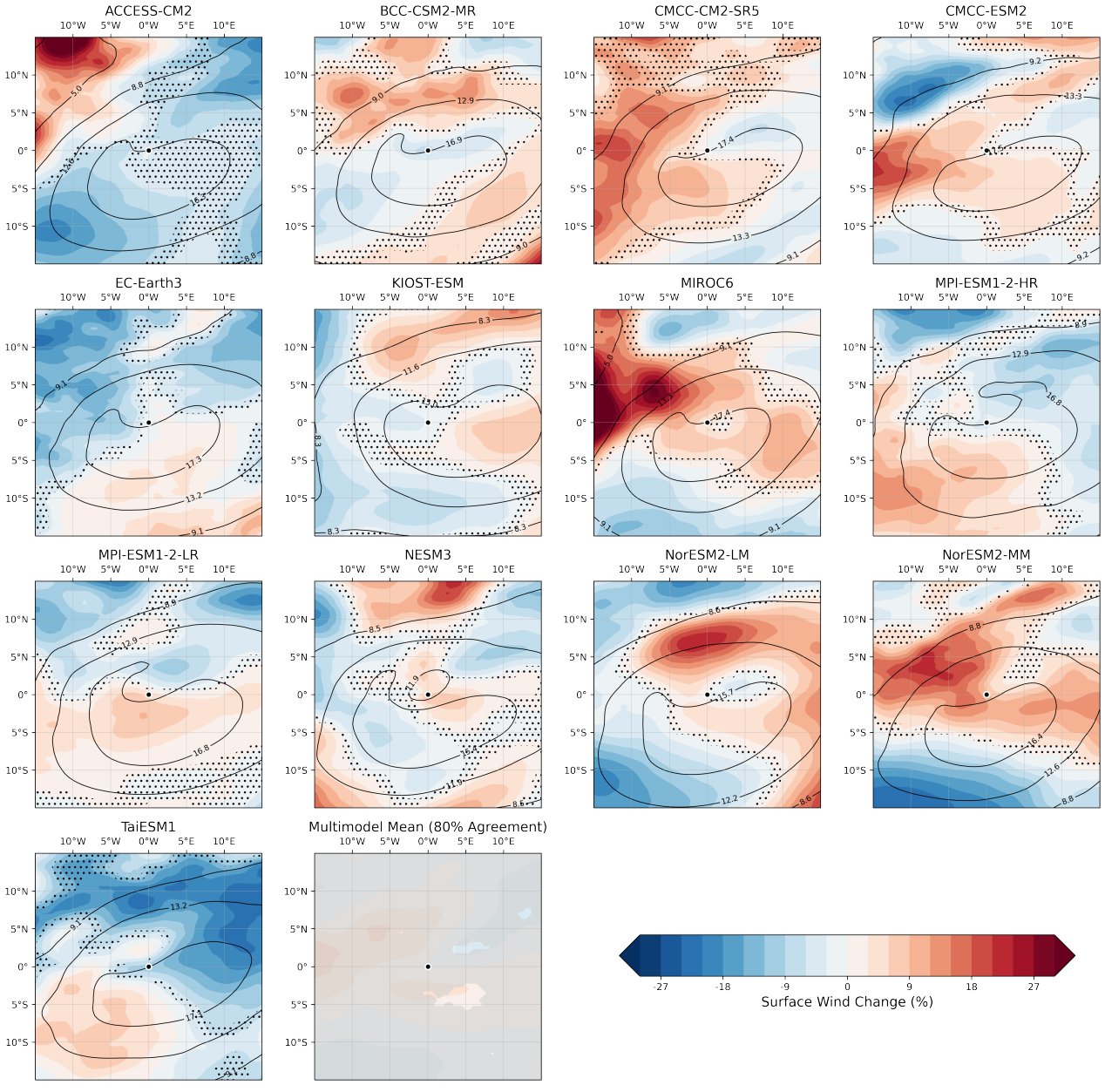

Figure 5. Cyclone-centered composite maps of percentage change in surface wind speed between SSP5-8.5 (2070–2100) and historical (1980–2010) periods for 13 CMIP6 models. The bottom-right panel shows the multimodel mean (MMM); shaded regions show where less than 80% of models agree on the sign of change. The cyclone center is marked with a black dot. Each subplot shows a $30^\circ \times 30^\circ$ domain centered on the cyclone, with longitude on the x-axis and latitude on the y-axis. Dots indicate regions without statistical significance at the 5% level.

https://doi.org/10.5194/egusphere-2026-1805
Preprint. Discussion started: 20 April 2026

cyclones, with coarser-resolution models tending to underestimate mesoscale wind features (Willison et al., 2013). Combined with the fact that warm-conveyor-belt-related wind accelerations are primarily expressed in the lower to mid-troposphere, rather than in the surface layer, these processes contribute to the muted and model-dependent surface wind signal. The multimodel mean (MMM) panel reflects this large inter-model spread. It shows only weak and spatially incoherent changes, with no clear pattern of either strengthening or weakening across the ensemble. Shaded regions in the MMM indicate areas where model agreement on the sign of change is low, highlighting the limited robustness of the surface wind response in CMIP6.

The diversity in model response potentially reflects differences in model resolution across the CMIP6 models (Table 1). Surface wind speed in extratropical cyclones is tightly constrained by the representation of the pressure gradients and pressure minimahich is known to be limited in coarse-resolution models even with a model grid spacing of approximately $0.7°$ to $2.5°$, (Priestley and Catto, 2022b; Roberts et al., 2020). While no strict theoretical resolution threshold exists, practical experience from numerical weather prediction indicates that kilometre-scale resolution is required for winds to be sufficiently resolved. As a result, model resolution may impose an effective upper-limit for simulated wind intensification, contributing to the spread seen across the ensemble.

Notably, models exhibiting strong precipitation increases do not necessarily show wind intensification. This decoupling suggests that enhanced latent heating primarily amplifies the hydrological footprint of extreme ETCs, while dynamical intensification remains constrained by competing effects such as reduced baroclinicity, changes in lower-level flow, and resolution-dependent limitations in simulating cyclone-related surface winds.

In addition, our analysis framework, where model outputs are interpolated to a common grid, may further attenuate systematic differences in wind responses by smoothing sharp pressure gradients and peak wind signals. This procedure, while necessary for inter-model comparability, may reduce signals that are intrinsically sensitive to horizontal resolution, potentially obscuring coherent resolution-dependent behavior (Schaffer et al., 2025).

Taken together, these results indicate that thermodynamic and dynamical aspects of extreme ETC structure respond to warming in independent ways. Increased precipitation emerges as a robust and coherent signal, whereas changes in surface winds and baroclinicity (as represented by the absolute temperature gradients) remain model-dependent and regionally variable, and is sensitive to model resolution and analysis methodology.

3.4 Shifts in the spatial distribution of peak intensity

Beyond changes in intensity and structure, extreme ETCs exhibit notable spatial redistribution under warming, potentially leading to implications for regional risk assessment. Such changes in storm track spatial distribution can occur due to dynamical and thermodynamic processes, including variations in moisture availability, diabatic heating along the warm conveyor belt, and modifications to near-surface baroclinicity and upper-level large-scale circulation, all of which vary across the North Atlantic and can influence the regions where cyclones most efficiently amplify. However, the magnitude and exact pattern of spatial redistribution vary considerably across models, emerging as a key source of uncertainty.

Figure 6 shows the zonal distribution of cyclone tracks across the North Atlantic, extending from $80°$W to $20°$E. For the 99th percentile events, counts typically range from 0 to approximately 10 events per longitude bin across all models and periods.

https://doi.org/10.5194/egusphere-2026-1805
Preprint. Discussion started: 20 April 2026

The majority of models display maxima in the historical period between 60°W and 40°W, corresponding to the western and central North Atlantic.

It is important to note that the 99th percentile event counts are calculated per period and per model. Since the total number of cyclone tracks generally decreases in the future period (as shown by the orange dashed lines representing all tracks), the absolute counts of 99th percentile events also tend to decrease, even when their relative frequency or spatial distribution may shift. This reduction in overall cyclone activity provides the context for interpreting changes in the extreme event distributions discussed below.

Seven models (CMCC-CM2-SR5, CMCC-ESM2, MIROC6, MPI-ESM1-2-HR, NESM3, NorESM2-MM, TaiESM1) show enhanced 99th percentile cyclone activity eastward of 50°W with reduced activity westward of 50°W, demonstrating an eastward redistribution of cyclone activity. Five models (ACCESS-CM2, EC-Earth3, KIOST-ESM, MPI-ESM1-2-LR, NorESM2-LM) exhibit mixed longitudinal changes without systematic directional shifts, with increases and decreases distributed across multiple longitude bands. One model (BCC-CSM2-MR) shows a westward shift, characterized by enhanced extreme-cyclone activity west of 50°W and reduced counts to the east.

The multi-model ensemble reveals greater inter-model spread in zonal changes than in other aspects of cyclone response. While the mean signal points toward an eastward redistribution of extreme cyclone intensity locations, substantial uncertainty remains regarding the magnitude and precise location of these shifts. Each panel also reports the Kolmogorov–Smirnov (KS) statistic and associated p-value, quantifying whether the longitudinal distribution of peak-intensity cyclones differs significantly between the historical and SSP5-8.5 periods. The KS results emphasize this spread: a number of models show statistically distinguishable historical and future distributions, while others exhibit changes that fall within sampling variability, underscoring that spatial redistribution is one of the least robust aspects of future ETC change. In addition, the large p-values indicate a majority of statistically non-significant shift in the zonal distribution between periods.

Figure 7 illustrates the latitudinal distribution of cyclone peak intensities across the North Atlantic. Most models exhibit maxima in the historical period between 45°N and 55°N, corresponding to the mid-latitude storm track region.

Three models (MIROC6, NESM3, NorESM2-LM) show northward displacement of extreme cyclone peak intensity locations, with enhanced activity at higher latitudes and reduced activity in the southern portion of the domain. Eight models (ACCESS-CM2, BCC-CSM2-MR, CMCC-CM2-SR5, CMCC-ESM2, EC-Earth3, KIOST-ESM, MPI-ESM1-2-HR, NorESM2-MM) exhibit mixed latitudinal signals without systematic directional shifts, showing amplitude changes or redistribution across multiple latitude bands. Two models (MPI-ESM1-2-LR, TaiESM1) show southward shifts, with enhanced activity at lower latitudes.

The ensemble displays substantial inter-model diversity in the latitudinal response, with models projecting either northward or southward shifts, or no clear latitudinal displacement. This spread highlights considerable uncertainty in projecting meridional changes in extreme North Atlantic cyclone activity under future warming.

https://doi.org/10.5194/egusphere-2026-1805
Preprint. Discussion started: 20 April 2026

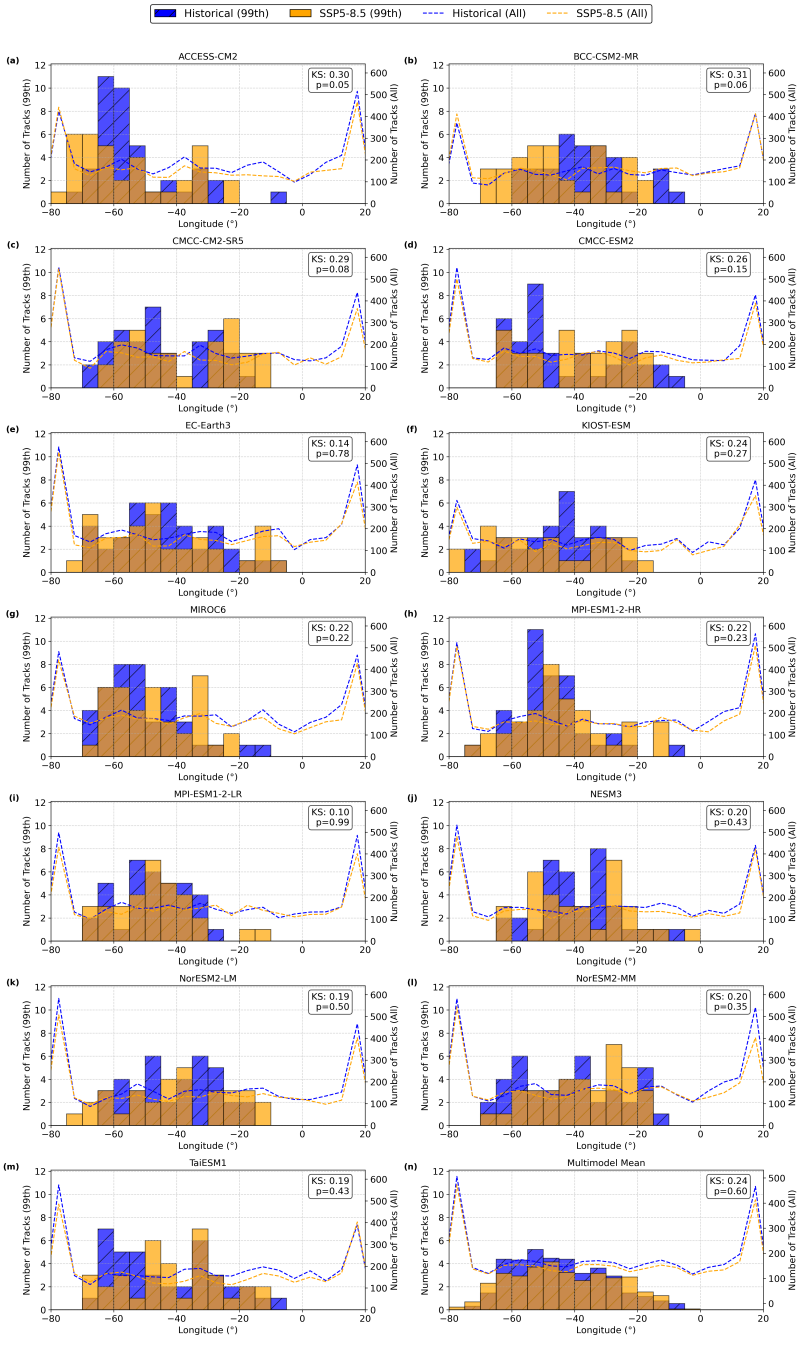

Figure 6. Zonal distribution of cyclone tracks for historical (1980–2010) and future (2070–2100, SSP5-8.5). Bars represent the 99th percentile most intense cyclones in the historical period (blue hatched) and in the future period (orange). Dashed lines show total cyclone counts for historical (blue) and future (orange). Distributions are for the North Atlantic domain (30°N–70°N, −80° to 20°).

https://doi.org/10.5194/egusphere-2026-1805
Preprint. Discussion started: 20 April 2026

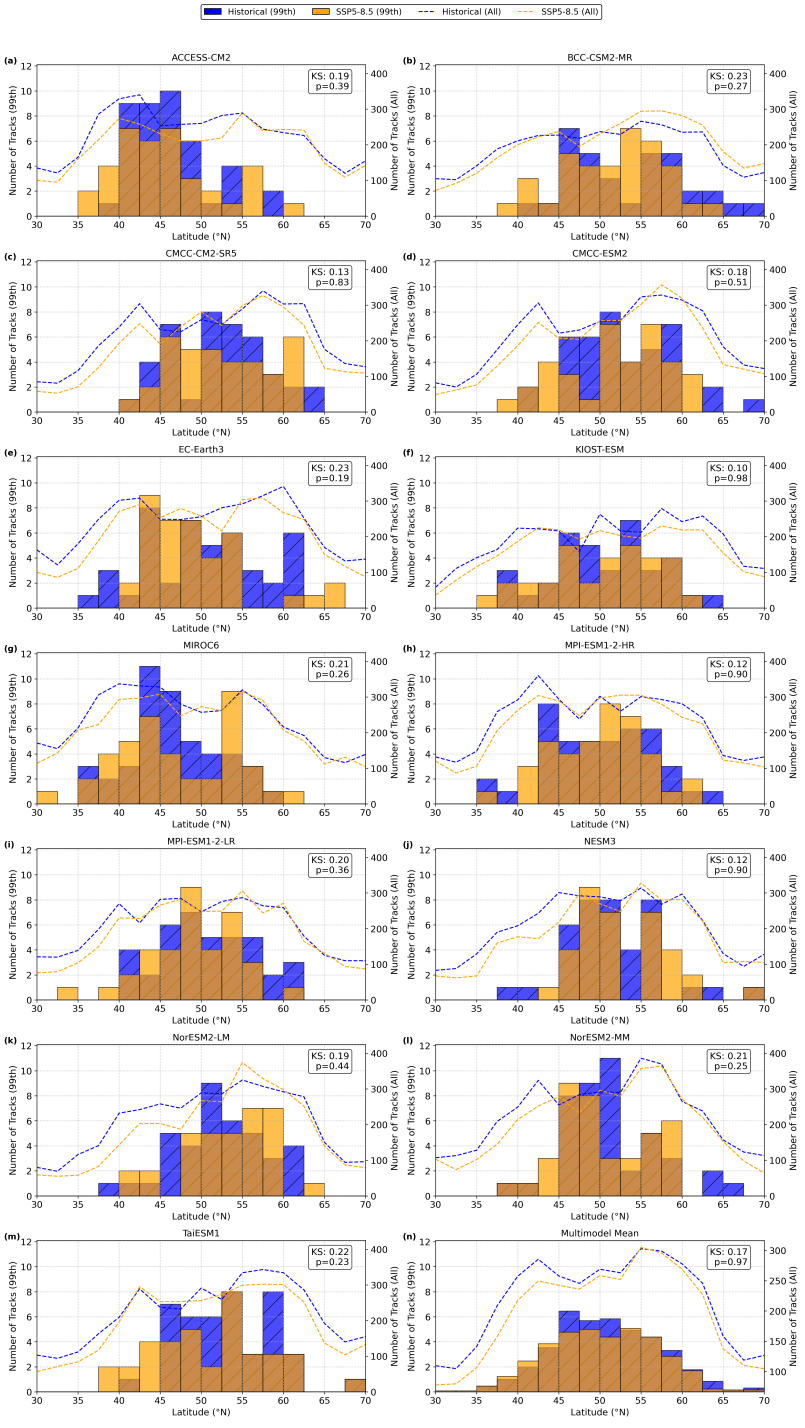

Figure 7. Latitudinal distribution of cyclone tracks for historical (1980–2010) and future (2070–2100, SSP5-8.5). Bars represent the 99th percentile most intense cyclones in the historical period (blue hatched) and in the future period (orange). Dashed lines show total cyclone counts for historical (blue) and future (orange). Distributions are for the North Atlantic (30°N–70°N, −80°W to 20°E).

https://doi.org/10.5194/egusphere-2026-1805
Preprint. Discussion started: 20 April 2026

4 Discussion and Conclusion

Future climate projections predict an extension of the wintertime storm track further into Europe posing a potential for increased risk under climate change, especially in winter. However, model uncertainty is considerable, making it difficult to robustly assess future surface weather response, including precipitation and surface winds.

In this study, we investigate the changes in the strength of extreme extratropical cyclones in the North Atlantic, with the goal of clarifying inter-model uncertainty. We focus on the top 100 strongest cyclones, identified according to their intensity. To better understand the large spread among climate models in projected cyclone intensity changes, we analyze the future response of individual models, rather than solely considering the multi-model mean.

Our analysis focuses specifically on peak vorticity locations rather than cyclone genesis regions or full track positions. While in literature there is generally an agreement regarding the northward and eastward shifts of extratropical cyclone tracks (Chang, 2016; Tamarin and Kaspi, 2016; Zappa et al., 2013), our analysis reveals more complex spatial patterns. The location where a cyclone reaches its peak vorticity may respond differently to climate change than its genesis location, as intensification processes depend on local environmental conditions, such as moisture availability, baroclinicity, and oceanic heat fluxes (Pfahl et al., 2015a). These conditions do not necessarily change in the same way as the mean storm track. For example, regions of enhanced low-level baroclinicity may persist or even intensify in localized areas due to SST gradients, while moisture availability and diabatic heating can shift independently of storm genesis patterns. As a result, the environmental conditions that are most favorable for rapid intensification of extratropical cyclones may migrate differently than the storm tracks (Pfahl et al., 2015a; Woollings et al., 2012). Seven out of thirteen models show robust eastward shifts in peak vorticity locations, consistent with mean storm track shifts. However, there is a substantial diversity in latitudinal responses, indicating that peak intensity locations may not simply follow the general poleward migration of storm tracks. This distinction is important because impacts are often greatest where cyclones reach their maximum intensity.

The eastward shift is consistent with projected changes in North Atlantic SST gradients and the position of oceanic frontal zones (Woollings et al., 2012; Kwon et al., 2010). The latitudinal diversity suggests that meridional shifts are more uncertain and potentially more sensitive to model-specific factors. Barnes and Polvani (2013) argued that while theory predicts poleward storm track migration, regional responses can deviate substantially from zonal mean expectations due to land-sea contrasts, topography, and stationary wave patterns. The southward shifts in NorESM2-MM, MPI-ESM1-2-LR, and TaiESM1 challenge the simple poleward migration narrative.

The substantial inter-model spread found in CMIP6 models suggests that model/internal variability is relatively high and that key physical processes remain poorly constrained. This could reflect genuine uncertainty about future climate states or varying model fidelity in representing critical processes (Priestley et al., 2020). While we observe consistent decreases in total cyclone frequency, our analysis does not address whether specific historical extreme cyclones have future analogues or whether entirely different synoptic patterns produce future top-100 events (Priestley and Catto, 2022a).

A critical limitation concerns the ability of coarse-resolution CMIP6 models to represent fine-scale structures in extreme cyclones. Model resolutions range from approximately 0.7° to 2.5° (80–280 km), while resolutions coarser than 1° struggle to

https://doi.org/10.5194/egusphere-2026-1805
Preprint. Discussion started: 20 April 2026

capture steep pressure gradients and wind maxima in the most intense cyclones (Knutson et al., 2013). Zeitzen et al. (2025) demonstrated that convection-permitting resolution (2 km) is necessary to accurately represent wind speed maxima and their fine-scale spatial structure, revealing that intensification manifests mainly in narrow bands of enhanced vorticity rather than broad-scale circulation changes. This suggests CMIP6 models may underestimate intensification magnitude, particularly for surface winds and resolution has been shown to strongly influence the representation and projected changes of cyclones with sting jets (Martín et al., 2023) and localized vorticity maxima (Michaelis et al., 2017). Specifically, the uncertainty found for surface wind speed (i.e., changes ranging from -15% to $+30\%$) may partially reflect resolution-dependent representation of boundary layer processes rather than genuine physical uncertainty (Willison et al., 2013; Priestley and Catto, 2022b). Higher-resolution simulations are needed to determine whether model disagreement represents true climate response uncertainty or resolution artifacts.

A promising direction for future research include large ensembles of future projections and high-resolution modeling. An assessment on the role of internal variability in climate model ensemble, as demonstrated in this study for the MPI-ESM1-2-LR large ensemble (Fig. 2b), would have important benefits for understanding and reducing uncertainty in future projections of weather extremes, including extreme cyclones. Additionally, future research should pursue high-resolution modeling and expanded large-ensemble experiments to better quantify the contribution of internal variability to projected ETC changes. Such work would help determine whether inter-model spread primarily reflects model physics or internal variability at convection-permitting scales ($\leq$2 km) to explicitly resolve fine-scale structures governing peak winds and localized intensification (Zeitzen et al., 2025). Such simulations would clarify whether inter-model spread reflects genuine physical uncertainty or insufficient resolution (Michaelis et al., 2017). Complementary machine learning approaches for statistical downscaling and improved parameterizations offer alternative strategies for translating coarse projections into actionable impact assessments (Brenowitz and Bretherton, 2018). Furthermore, systematic investigation of extreme cyclone energetics, such as process analysis separating dry from moist dynamics, can help to further clarify the relative importance of dry baroclinic versus moist diabatic processes (Binder et al., 2023; Auestad et al., 2025).

Data availability. The CMIP6 data can be obtained from the ESGF website: https://wcrp-cmip.org/cmip-data-access. ERA5 reanalysis dataset (Hersbach et al., 2020) is freely available through the Copernicus Climate Change Service (Copernicus Climate Change Service, 2023).

Code and data availability. Cyclone track datasets and other diagnostic code are available from the corresponding authors upon request.

https://doi.org/10.5194/egusphere-2026-1805
Preprint. Discussion started: 20 April 2026

Author contributions. H.A.G. and L.M. designed the study. M.P. provided the model data, and L.M. performed the analysis, prepared the figures and wrote the first version of the manuscript. All authors contributed to the work process, interpretation of the results and to the writing of the manuscript.

Competing interests. The authors declare that no competing interests are present.

Acknowledgements. Support from the Swiss National Science Foundation through project PZ00P2_223676 to H.A.G is gratefully acknowledged.

https://doi.org/10.5194/egusphere-2026-1805
Preprint. Discussion started: 20 April 2026

References

Auestad, H., Shibu, A., Ceppi, P., and Woollings, T.: The latent heating feedback on the mid-latitude circulation, Geophysical Research Letters, 52, e2025GL116 437, 2025.

Barnes, E. A. and Polvani, L. M.: Response of the midlatitude jets, and of their variability, to increased greenhouse gases in the CMIP5 models, Journal of Climate, 26, 7117–7135, https://doi.org/10.1175/JCLI-D-12-00536.1, 2013.

Binder, H., Boettcher, M., Grams, C., Joos, H., Pfahl, S., and Wernli, H.: Exceptional air mass transport and dynamical drivers of an extreme wintertime Arctic warm event, Geophysical Research Letters, 50, e2022GL101 638, https://doi.org/10.1029/2022GL101638, 2023.

Blackmon, M. L.: A climatological spectral study of the 500 mb geopotential height of the Northern Hemisphere, J. Atmos. Sci., 33, 1607–1623, 1976.

Brenowitz, N. D. and Bretherton, C. S.: Prognostic validation of a data-driven parameterization for subgrid processes, Geophysical Research Letters, 45, 6289–6298, https://doi.org/10.1029/2018GL078510, 2018.

Catto, J. L., Winton, M., and Palmer, T. N.: The future of midlatitude cyclones, Current Climate Change Reports, 5, 407–420, https://doi.org/10.1007/s40641-019-00149-4, 2019.

Chang, E. K.: CMIP5 projection of significant reduction in extratropical cyclone activity over North America, Journal of Climate, 29, 2163–2182, https://doi.org/10.1175/JCLI-D-15-0501.1, 2016.

Copernicus Climate Change Service: ERA5 hourly data on pressure levels from 1940 to present, Copernicus Climate Change Service (C3S) Climate Data Store (CDS) [data set], https://doi.org/10.24381/cds.bd0915c6, 2023.

Hersbach, H., Bell, B., Berrisford, P., Hirahara, S., Horányi, A., Muñoz-Sabater, J., Nicolas, J., Peubey, C., Radu, R., Schepers, D., et al.: The ERA5 global reanalysis, Quarterly Journal of the Royal Meteorological Society, 146, 1999–2049, https://doi.org/10.1002/qj.3803, 2020.

Hodges, K. I.: A general method for tracking analysis and its application to meteorological data, Monthly Weather Review, 122, 2573–2586, https://doi.org/10.1175/1520-0493(1994)122<2573:AGMFTA>2.0.CO;2, 1994.

Hodges, K. I.: Feature tracking on the unit sphere, Monthly Weather Review, 123, 3458–3465, https://doi.org/10.1175/1520-0493(1995)123<3458:FTOTUS>2.0.CO;2, 1995.

Hodges, K. I.: Adaptive constraints for feature tracking, Monthly Weather Review, 127, 1362–1373, https://doi.org/10.1175/1520-0493(1999)127<1362:ACFT>2.0.CO;2, 1999.

Hoskins, B. and Valdes, P.: On the existence of storm-tracks, J. Atmos. Sci., 47, 1854–1864, 1990.

Karpechko, A. Y., Afargan-Gerstman, H., Butler, A. H., Domeisen, D. I., Kretschmer, M., Lawrence, Z., Manzini, E., Sigmond, M., Simpson, I. R., and Wu, Z.: Northern hemisphere stratosphere-troposphere circulation change in CMIP6 models: 1. Inter-model spread and scenario sensitivity, Journal of Geophysical Research: Atmospheres, 127, e2022JD036 992, 2022.

Knutson, T. R., Sirutis, J. J., Zhao, M., Tuleya, R. E., Bender, M., Vecchi, G. A., Villarini, G., and Chavas, D.: Dynamical downscaling projections of twenty-first-century Atlantic hurricane activity: CMIP3 and CMIP5 model-based scenarios, Journal of Climate, 26, 6591–6617, https://doi.org/10.1175/JCLI-D-12-00539.1, 2013.

Kwon, Y.-O., Alexander, M. A., Bond, N. A., and Overland, J. E.: Role of the Gulf Stream northern wall and North Atlantic Oscillation in the winter eddy-driven jet variability, Journal of Geophysical Research: Atmospheres, 115, D21 120, https://doi.org/10.1029/2010JD014336, 2010.

Laïne, M., Joos, H., Forbes, R., Sodemann, H., and Wernli, H.: Diabatic processes and life cycle of an extratropical cyclone in a warm conveyor belt, Monthly Weather Review, 137, 3404–3423, https://doi.org/10.1175/2009MWR2855.1, 2009.

https://doi.org/10.5194/egusphere-2026-1805
Preprint. Discussion started: 20 April 2026

Little, A. S., Priestley, M. D., and Catto, J. L.: Future increased risk from extratropical windstorms in northern Europe, Nature Communications, 14, 4434, 2023.

Manzini, E., Karpechko, A. Y., Anstey, J., Baldwin, M., Black, R., Cagnazzo, C., Calvo, N., Charlton-Perez, A., Christiansen, B., Davini, P., et al.: Northern winter climate change: Assessment of uncertainty in CMIP5 projections related to stratosphere-troposphere coupling, Journal of Geophysical Research: Atmospheres, 119, 7979–7998, 2014.

Martín, A., Roberts, M. J., Vidale, P. L., Hodges, K., Vannière, B., Demory, M.-E., and Seddon, J.: The role of model resolution in simulating sting-jet-producing cyclones: insights from high-resolution modelling experiments, Climate Risk Management, 41, 100 570, https://doi.org/10.1016/j.crm.2023.100570, 2023.

Michaelis, A. C., Lackmann, G. M., and Robinson, W. A.: Changes in winter North Atlantic extratropical cyclones in high-resolution regional pseudo–global warming simulations, Journal of Climate, 30, 6905–6925, https://doi.org/10.1175/JCLI-D-16-0697.1, 2017.

Oudar, T., Cattiaux, J., and Douville, H.: Drivers of the Northern Extratropical Eddy-Driven Jet Change in CMIP5 and CMIP6 Models, Geophysical Research Letters, 47, e2019GL086 695, 2020.

Pfahl, S., O'Gorman, P. A., and Singh, M. S.: Extratropical cyclones in idealized simulations of changed climates, Journal of Climate, 28, 9373–9392, https://doi.org/10.1175/JCLI-D-14-00816.1, 2015a.

Pfahl, S., Schwierz, C., Croci-Maspoli, M., Grams, C. M., and Wernli, H.: Importance of latent heat release in ascending air streams for atmospheric blocking, Nature Geoscience, 8, 610–614, 2015b.

Pfahl, S., Schwierz, C., Croci-Maspoli, M., Grams, C. M., and Wernli, H.: Importance of latent heat release in ascending air streams for atmospheric blocking, Nature Geoscience, 8, 610–614, https://doi.org/10.1038/ngeo2487, 2015c.

Pinto, J. G., Fröhlich, E. L., Leckebusch, G. C., and Ulbrich, U.: Changing European storm loss potentials under modified climate conditions according to ensemble simulations of the ECHAM5/MPI-OM1 GCM, 7, 165–175, https://doi.org/10.5194/nhess-7-165-2007, 2007.

Priestley, M., Ackerley, D., Catto, J., Hodges, K., McDonald, R., and Lee, R.: An overview of the extratropical storm tracks in CMIP6 historical simulations, Journal of Climate, 33, 6315–6343, https://doi.org/10.1175/JCLI-D-19-0928.1, 2020.

Priestley, M., Ackerley, D., Catto, J., and Hodges, K.: Drivers of biases in the CMIP6 extratropical storm tracks. Part I: Northern Hemisphere, Journal of Climate, 36, 1451–1467, https://doi.org/10.1175/JCLI-D-22-0263.1, 2023.

Priestley, M. D. and Catto, J. L.: Future changes in the extratropical storm tracks and cyclone intensity, wind speed, and structure, Weather and Climate Dynamics, 3, 337–360, https://doi.org/10.5194/wcd-3-337-2022, 2022a.

Priestley, M. D. and Catto, J. L.: Improved representation of extratropical cyclone structure in HighResMIP models, Geophysical Research Letters, 49, e2021GL096 708, 2022b.

Roberts, M. J., Camp, J., Seddon, J., Vidale, P. L., Hodges, K., Vanniere, B., et al.: Impact of model resolution on tropical cyclone simulation using the HighResMIP–PRIMAVERA multimodel ensemble, Journal of Climate, 33, 2557–2583, 2020.

Schaffer, A., Lichtenegger, T., Ossó, A., and Maraun, D.: Resolution dependence and biases in cold and warm frontal heavy precipitation over Europe in CMIP6 and EURO-CORDEX models, Weather and Climate Dynamics, 6, 1815–1830, 2025.

Screen, J. A. and Simmonds, I.: Amplified mid-latitude planetary waves favour particular regional weather extremes, Nature Climate Change, 4, 704–709, https://doi.org/10.1038/nclimate2271, 2014.

Severino, L. G., Kropf, C. M., Afargan-Gerstman, H., Fairless, C., de Vries, A. J., Domeisen, D. I., and Bresch, D. N.: Projections and uncertainties of winter windstorm damage in Europe in a changing climate, Natural Hazards and Earth System Sciences, 24, 1555–1578, 2024.

https://doi.org/10.5194/egusphere-2026-1805
Preprint. Discussion started: 20 April 2026

Shaw, T. A., Baldwin, M., Barnes, E. A., Caballero, R., Garfinkel, C. I., Hwang, Y.-T., Li, C., O'Gorman, P. A., Rivière, G., Simpson, I. R., and Voigt, A.: Storm track processes and the opposing influences of climate change, Nature Geoscience, 9, 656–664, https://doi.org/10.1038/ngeo2783, 2016.

Tamarin, T. and Kaspi, Y.: The poleward motion of extratropical cyclones from a potential vorticity tendency analysis, J. Atmos. Sci., 73, 1687–1707, 2016.

Vallis, G.: Atmospheric and oceanic fluid dynamics: Fundamentals and large-scale circulation, 2007.

Wernli, H. and Schwierz, C.: Surface cyclones in the ERA-40 dataset (1958–2001). Part I: Novel identification method and global climatology, Journal of the Atmospheric Sciences, 63, 2486–2507, 2006.

Willison, J., Robinson, W., and Lackmann, G.: The importance of resolving mesoscale latent heating in the North Atlantic storm track, Journal of the Atmospheric Sciences, 70, 2234–2250, https://doi.org/10.1175/JAS-D-12-0226.1, 2013.

Woollings, T., Gregory, J. M., Pinto, J. G., Reyers, M., and Brayshaw, D. J.: Response of the North Atlantic storm track to climate change shaped by ocean–atmosphere coupling, Nature Geoscience, 5, 313–317, https://doi.org/10.1038/ngeo1438, 2012.

Zappa, G. and Shepherd, T. G.: Storylines of atmospheric circulation change for European regional climate impact assessment, Journal of Climate, 30, 6561–6577, 2017.

Zappa, G., Shaffrey, L. C., Hodges, K. I., Slingo, J. M., and Fischer, E. M.: A multimodel assessment of future projections of North Atlantic and European extratropical cyclones in the CMIP5 climate models, Journal of Climate, 26, 5846–5862, https://doi.org/10.1175/JCLI-D-12-00573.1, 2013.

Zeitzen, R. M., Christensen, J. H., Øelund, J., Feddersen, H., Vedel, H., Nielsen, N. W., and Matte, D.: Windstorm extremes in a warmer world: Raising the bar for destruction, Geophysical Research Letters, 52, e2025GL115 936, https://doi.org/10.1029/2025GL115936, 2025.